Traffic-Aware Optical Network Growth Techniques

RASOUL SADEGHI[1,*], ROBIN MATZNER[1], YI-ZHI XU[2], ALEJANDRA BEGHELLI[1], DAVID SAAD[3], AND POLINA BAYVEL[1]

[1] Optical Networks Group, Department of Electronic and Electrical Engineering, University College London, Roberts Building, Torrington Place, London WC1E 7JE, UK
[2] Institute of Intelligent Computing, University of Electronic Science and Technology of China, Chengdu 611731, China
[3] College of Engineering and Physical Sciences, Aston University, Birmingham B4 7ET, UK
[*] r.yamchi@ucl.ac.uk

Compiled July 18, 2025

Maximising network throughput is crucial for operators facing rapid traffic growth. One effective strategy for achieving this is through targeted network expansion - strategically adding edges to maximise network throughput, not only for a specific set of demands but also for future traffic growth. Finding the optimal combination of new edges to maximise throughput is a NP-hard optimisation problem. Therefore, in this work, we propose four novel scalable network expansion methods that consider the network traffic distribution, and the network physical and structural properties to select the edges to be added to the optical infrastructure. The proposed methods belong to either the Cut Set category or the Cut Set and message passing combinations (Hybrid) category. The Cut Set methods aim to add new edges that eliminate structural bottlenecks in the network, prioritising either those that decrease path length or increase Signal to Noise Ratio (SNR). The Hybrid methods leverage the strengths of both message-passing and Cut Set approaches by strategically selecting new edges to reduce path lengths through message passing while targeting bottlenecks with the Cut Set technique. We applied these methods to 100 NFSNet-based synthetic graphs and 44 real-world topologies and evaluated their performance against two baseline methods previously evaluated in the literature. Numerical results show that the proposed methods outperform the baseline approaches, that methods taking the SNR into account perform better than those considering path lengths and that topology properties significantly impact the performance of proposed network expansion methods.

http://dx.doi.org/10.1364/ao.XX.XXXXXX

1. INTRODUCTION

The exponential growth of cloud-based applications, high-definition streaming, virtual and augmented reality, and the ongoing deployment of 5G/6G networks and AI continue to drive the demand for higher throughput in optical networks which underpin the digital communications infrastructure [1]. These evolving requirements necessitate innovative solutions to enhance optical network performance. These include: (1) increase the optical bandwidth within the existing fibre infrastructure, referred to as the ultrawideband regime [2–5], and (2) expansion of the network infrastructure itself through the addition of new optical fibre links or the lighting of existing dark fibres between cities/nodes [6–10]. The challenge in the latter lies in identifying the links which maximise the overall network throughput, for any given growth in traffic demand. This problem is an NP-hard combinatorial optimisation problem due to the large number of candidate edges in optical networks [11]. It is compounded by the fact that network throughput depends on the solution of the routing and wavelength assignment (RWA) problem, also a NP-hard problem [11].

Simple greedy heuristic methods, which make locally optimal choices at each step, often result in inefficiencies through not considering the global optimum, leading to resource bottlenecks. In recent years, however, researchers have explored more sophisticated approaches, integrating physical layer properties and structural/graph-theoretic attributes to optimise network topologies in terms of throughput and resource utilization [12, 13], as well as leveraging artificial intelligence (AI) techniques. For example, in [14], the authors utilise graph embeddings processed by a machine learning classifier for edge predic-

tion. Another method for network growth, specifically tailored for spatial networks, uses a Monte Carlo tree search (MCTS) framework to add the most beneficial links to the topology [15]. Zhang *et. al.* [16] developed graph neural network (GNN) methods for link prediction in a graph, which focus on predicting the existence of links between nodes in various types of networks. These methods address the limitations of traditional heuristics using GNNs to jointly learn from graph structure and node/edge features, enhancing prediction accuracy gradually over the years. However, the complexity of GNNs can pose challenges to generalizability, particularly when applied to networks with varying structures or unpredictable growth patterns. The studies above focused on the graph-theoretic properties of networks without taking into account the physical properties of the fibre links and optical networks or traffic dynamics specific to optical networks. Given that both traffic distributions and physical properties impact network throughput, it is important to incorporate these [17–19]. To this end, Xu *et al.* [20] developed a probabilistic optimisation framework for network pruning and growth, specifically tailored to optical networks. This approach is based on Message Passing (MP)-techniques to optimise the removal and addition of network edges. These techniques aim to minimise the total path length, given a specific traffic demand. By minimising the path length, network throughput is expected to be maximised. In our previous work, we compared the MP variant 1 based method proposed in [20] against the demand weighted cost (DWC) approach for expanding optical networks, deliberately excluding physical layer properties such as nonlinearity [21].

Building on this foundation, in this paper, we extend our earlier research by incorporating nonlinear effects into the optical network growth process. Four new methods are proposed for optical network topology growth under a given traffic demands, namely: Cut Set General (CS-G), Cut Set SNR (CS-SNR), Message Passing Variant 3 plus CS General (MP3 + CS-G) and Message Passing Variant 3 plus CS SNR (MP3 + CS-SNR). The first two are based on Cut Set approaches and the last two are hybrid methods combining Cut Set approaches with a message-passing technique. All of them include, for the first time, the physical properties of optical networks such as SNR. Their performance was evaluated and compared against two baseline methods: DWC-based and MP-based (variant 1 of the MP) methods [21].

The remainder of this paper is organized as follows: Section 2 introduces the network modelling and explains the proposed network growth methods. Section 3 evaluates the proposed methods using synthetic network topologies and real-world network topologies to quantify the maximum achievable throughput of established demands, Section 4 gives a summary of findings and suggestions for future research directions. Finally, Appendix A presents additional information on message passing and discusses further novel expansion approaches not included in the main discussion due to their inferior performance.

2. THE NETWORK MODEL AND EXPANSION METHODS

The optical network is represented as a graph $G(V, E)$, where V denotes the set of nodes, $V \equiv \{i \mid i \in V\}$, and E represents the set of edges, $E \equiv \{(i, j) \mid (i, j) \in V \times V\}$. Each edge corresponds to a standard single mode fiber (SSMF) link that supports W wavelengths in the C-band. Erbium-Doped Fiber Amplifiers (EDFAs) with a noise figure $NF = 4.5dB$ are assumed to be deployed after each span, with a number of spans denoted by N_s with span length $L_s = 80km$. Each node in this network represents a routing node or a Reconfigurable Optical Add-Drop Multiplexer (ROADM), where traffic can be added, dropped, or passed through. The traffic demand between any node pair (i, j) is defined by the number of connections from the source node i to the destination node j, with each connection requiring one wavelength.

The network growth problem consists of identifying the set of k edges to be added to the topology, such that the throughput of the extended network topology is maximized for a given traffic demand.

The inputs to the network expansion methods proposed in this work are: **i)** the original network topology $G(V, E)$, **ii)** the traffic matrix D, which specifies the demand between each node pair (number of connections), and **iii)** the number of edges to be added, k. The final output is the set of k edges to be added to the topology.

In the following subsections, we describe the novel methods proposed in this work: CS-G and CS-SNR (Cut Set category) and MP3 + CS-G and MP3 + CS-SNR (hybrid category). For completeness, we also include the description of the baseline methods previously proposed in [21]: the DWC-based and MP1-based methods. Also, in appendix B less efficient methods, namely algebraic connectivity and MP2 based methods (MP Variant 2), are explained and compared.

A. Cut Set based methods

A network cut set is a set of links that separates the network into two disjoint subnetworks. A network can have many different cut sets. However, the cut set supporting the highest number of connections (the most congested cut set) is key for network throughput. This is because it accurately describes the number of wavelengths required to communicate these connections and therefore also estimates how many connections can be set up at maximum load. Thus, by adding links that increase the cardinality of the most congested cut set, a higher network throughput can be achieved. The network expansion methods based on the cut set concept operate as follows:

STEP 1: Identify the most congested cut set. The congestion of a cut set is equal to the number of connections passing through the edges connecting the disjoint subgraphs/subnetworks.

STEP 2: Find k new edges that connect the subnetworks separated by the most congested cut set.

To carry out STEP 1, two methods can be used: *Exhaustive Search* or *Simple Path Search* [22, 23]. The Exhaustive Search method systematically examines all possible partitions of the network nodes into two subnetworks and identifies the edges that, when removed, would disconnect the network, as shown in Fig. 1(a). This approach ensures that all potential cut sets are identified, but it is computationally intensive, struggling with networks with more than 30 nodes [23]. In contrast, the Simple Path Search method focuses on identifying cut sets by analysing loop-free (simple) paths, which do not revisit any node, between all node pairs. It determines which paths are critical to maintaining network connectivity. This method is more computationally efficient as it reduces the number of partitions that need to be evaluated while still identifying the most significant cut sets. For example, for a network topology with 14 nodes and 21 edges, the number of partitions that divide the network into two subnetworks is equal to 16382. Using the Simple Path method, the number of partitions decreases by about 70% to 1143. This reduction occurs because, in the Simple Path method, instead of

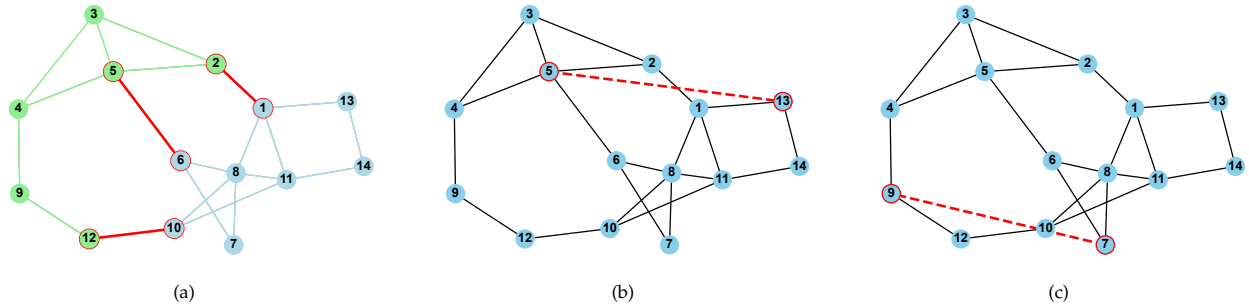

(a) (b) (c)

Fig. 1. (a) Cut set (red edges) found by an exhaustive search considering all-to-all demands (one connection per node-pair), **(b)** New edge added by the CS-G method for k=1, **(c)** New edge added by the CS-SNR method for k=1.

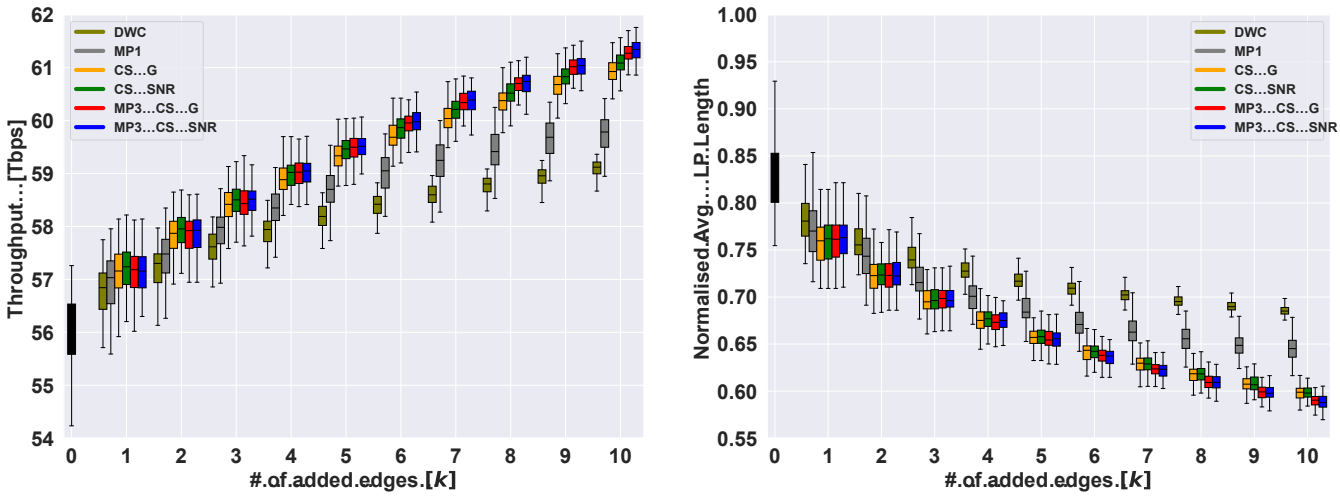

(a) (b)

Fig. 2. (a) Normalised average lightpath length and **(b)** network throughput versus k when applying the proposed and baseline algorithms in Scenario A to 100 NFSNet-based topologies.

considering all possible combinations, only the simple paths are calculated as candidates for the cut set.

In this work, both methods have been rigorously tested with more than 10,000 graphs, consistently yielding identical results. Depending on how STEP 2 is performed, two cut set based techniques are proposed:

- **Cut Set General (CS-G)**: Once the cut set edges have been identified (Fig. 1(a)) in STEP 1, STEP 2 is executed by using one candidate edge (edges that, when added to the graph, establish connections between previously disjoint components to make the graph fully connected) at a time, until k edges are added to the network. To select the next edge to be added to the topology, all edges connecting nodes in different subnetworks are evaluated based on their ability to minimise the average path length for the traffic. The edge that results in the greatest reduction in average path length is selected and added to the network. This procedure is repeated to identify and add the k most effective edges. Fig. 1(b) shows the edge identified by CS-G (dashed red) for $k = 1$.

- **Cut Set SNR (CS-SNR)**: This method, as CS-G, also identifies candidate edges that connect the two subnetworks separated by the most congested cut set. However, instead of selecting the edge that minimises the average path length, CS-SNR prioritises the edge that maximises the SNR of the uniform demands matrix. To this end, the Routing and Wavelength Allocation (RWA) problem is solved for the given traffic pattern for each candidate edge. The edge that improves the total SNR of the given demands the most, is chosen to be added to the topology. This process is repeated until k edges are added to the network. By maximising the SNR the quality of transmission of the optical signal is enhanced which, in turn, improves throughput. Fig. 1(c), shows the edge selected by CS-SNR (dashed red) at k=1, when the RWA problem is solved by applying the Shortest Path First Fit heuristic.

B. Hybrid methods

We propose two hybrid methods that combine an improved variant of the network expansion method based on MP presented in [20, 21] and the Cut Set methods discussed above. MP - also known as belief propagation - is a probabilistic method aimed at calculating the maximal marginal posterior of the system vari-

Table 1. Average throughput in Tbps for all methods across 100 initial graphs, with k edges added (ranging from 1 to 10) for the all to all traffic pattern. The capacity values reflect the performance of each method in optimising the network throughput. The initial 100 networks delivered capacity for all to all demands is equal to 56.01 Tbps.

k=	1	2	3	4	5	6	7	8	9	10
MP1	56.93	57.44	57.92	58.32	58.68	59	59.19	59.44	59.63	59.75
DWC	56.77	57.22	57.59	57.90	58.16	58.39	58.58	58.77	58.93	59.09
CS-G	57.16	57.83	58.39	58.88	59.33	59.71	60.04	60.35	60.65	60.93
CS-SNR	**57.20**	**57.92**	**58.49**	58.98	59.43	59.83	60.20	60.51	60.81	61.08
MP3 + CS-G	57.15	57.86	58.45	59.01	59.48	59.94	60.34	60.69	61.01	61.28
MP3 + CS-SNR	57.13	57.86	**58.49**	**59.03**	**59.50**	**59.98**	**60.36**	**60.70**	**61.02**	**61.32**

Table 2. Average lightpath length (measured in the number of spans), for all methods across 100 graphs, with k edges added (ranging from 1 to 10) for the all to all traffic pattern. The lightpath length values reflect the performance of each method in optimising the network lightpath length. the average lightpath length for the initial networks is equal to 41 spans.

k=	1	2	3	4	5	6	7	8	9	10
MP1	38.05	36.71	35.51	34.58	33.88	33.19	32.80	32.37	32.03	31.84
DWC	38.63	37.43	36.58	35.93	35.41	34.98	34.63	34.31	34.04	33.80
CS-G	**37.40**	**35.66**	**34.35**	33.28	32.36	31.62	31.02	30.46	29.96	29.52
CS-SNR	37.52	35.72	34.40	33.34	32.44	31.66	31.03	30.48	29.96	29.52
MP3 + CS-G	37.54	35.73	34.40	**33.18**	32.31	31.45	30.72	30.06	29.53	29.07
MP3 + CS-SNR	37.57	35.76	34.38	33.21	**32.27**	**31.37**	**30.68**	**30.03**	**29.48**	**29**

ables based on passing messages (conditional probabilities) from neighbouring interacting variables [24]. It has been adapted and applied to address non-localised optimisation problems such as routing in general [25, 26] and routing in optical communication [27] in particular. The algorithm follows a path for each assignment to optimise a global objective. The MP approach can be cast as a minimisation of a cost function (e.g., latency, throughput) under some problem constraints, such as that routing assignments must be contiguous from source to destination, adhere to edge-disjoint routing, etc. The difference between the different MP variants we consider are as follows: MP3 is an algorithm for network expansion under simple routing in the absence of interaction between outing assignments; MP1 and MP2 are variants of MP3 that force edge-disjoint routing assignments in multi-wavelengths RWA (such that the same wavelength cannot be allocated to two separate routing assignments on an edge); the difference between MP1 and MP2 is that the objective function in MP1 includes distances as cost weights, while MP2 considers SNR values as the edge weights. More details about the derivation and the rationale behind them can be found in Appendix A, section B. The hybrid methods named MP3 + CS-G and MP3 + CS-SNR they aim to maximise throughput by selecting the k edges from candidate edge set E_a that minimise the shortest path length for a given demand, following 2 steps:

STEP 1: Identify a set of E_a edges, with $E_a > k$, to be provisionally added to the topology. The provisionally extended topology is denoted by G'. MP3 + CS-G and MP3 + CS-SNR find the set of E_a edges by executing CS-G and CS-SNR, respectively.

STEP 2: Execute variant 3 (MP3) of the message-passing method to prune G' and retain only k edges from the E_a candidate edges.

C. Additional methods

We developed and evaluated three additional network expansion methods: (1) Algebraic Connectivity-based method, (2) MP Variant 2 with the objective of maximising the SNR. In this method the E_a edges are selected based on simple greedy method (MP2_SNR max) and (3) MP Variant 2 with the objective of maximising the SNR for the demands by using CS-G and CS-SNR to select the E_a candidate edges (MP2_SNR max + CS G, MP2_SNR max + CS SNR). None of them outperformed the cut set-based methods and hybrid methods discussed above. Hence, they are not discussed in this section or in the rest of the paper. For completeness, they are included in Appendix A.

D. Baseline methods

D.1. DWC-based method

This greedy method uses the DWC metric, demonstrated to be highly correlated with the inverse of network throughput [18], to select new edges. Given a topology and a set of traffic demands established according to a routing and RWA algorithm, the DWC metric is calculated as follow:

$$DWC = \sum_{z \in Z} \mathrm{T}_z \cdot (\alpha \cdot L_z + (1 - \alpha) \cdot H_z) \quad \textbf{(1)}$$

where Z represents the set of node pairs (source and destination), and T_z is the normalised traffic demand between node pair z. This demand is calculated by dividing the number of connections requested between the node pair D_z by the total number of connections across all node pairs, $\sum_{z \in Z} D_z$. Both L_z and H_z

correspond to the length and the number of hops of the shortest LP for the node pair z, respectively, which are highly dependent on the RWA algorithm used to establish the demands. α denotes the network's density and is defined as $\alpha = \frac{2|E|}{|V|(|V|-1)}$ [28], where $|E|$ and $|V|$ are the total number of edges and nodes in the network, respectively.

The DWC-based method works as follows. For each possible e edge that could be added to the network, the DWC metric is calculated. The edge that results in the lowest DWC value — indicating a potential maximum increase in network throughput — is selected. This selection process is repeated k times, corresponding to the number of new edges to be added.

The computational complexity of the DWC-based method is dominated by the k-shortest path algorithm, here implemented using Yen's algorithm with a complexity of $O(l \cdot |V|^3)$, where l is the number of k-shortest paths used $l = 5$. This calculation is performed for each potential edge ($\frac{|V|\cdot(|V|-1)}{2}$) and repeated for k edge additions, resulting in an overall complexity of $O(\frac{l\cdot k\cdot |V|^5}{2})$.

D.2. MP1

This approach, originally proposed in [20], uses the path length as a proxy for network throughput: the shorter the path lengths, the higher the throughput. Thus, it selects the k edges that contribute the most to decrease the average lightpath (LP) length for the given traffic demand, following 2 steps: In STEP 1, E_a edges are added to the graph, with $E_a > k$. To do so, each possible new edge is evaluated in terms of the resulting average path length of the demands after its eventual addition. The candidate edges are then ranked on the basis of their ability to reduce the average path length. The top $E_a = n$ edges — those that offered the greatest reduction in average path length — are then added to the provisional network topology $G' = G(V, E + E_a)$. In STEP 2, G' is input to an MP-based procedure that prunes $E_a - k$ edges from G' by applying a computationally efficient MP technique [20]. The pruning process is a probabilistic approach that relies on an approximate calculation of posterior marginals for edges to be removed based on a coupled optimisation of routing and topology. The computational complexity of this method is $O((|D| + W)|D|^2|E|Wk)$ where $|D|$, W, $|E|$ and k are the number of demands, wavelengths, network edges and added edges, respectively [20]. MP1 is similar to MP3, as explained in Sec. B, except for the additional edge-disjoint routing constraints on multi-wavelength networks, whereas in MP3 paths have no impact on one another. MP2 is a generalised variant of MP1, in which edge weight varies on different edges, representing SNR values to optimise throughput; more details can be found in App. B.2.

3. NETWORK PERFORMANCE EVALUATION

The performance of the proposed methods was evaluated in terms of the network throughput, NT, achieved by the expanded topology, calculated using the Shannon capacity formula:

$$NT = \sum_{z \in Z} 2 \cdot B \cdot \log_2(1 + SNR_z) \quad \textbf{(2)}$$

where B represents the channel bandwidth and SNR_z denotes the SNR of the lightpath allocated to demand z. We assume a network operating in the C-band frequency range (191-196 THz), supporting $W = 156$ channels per edge. Thus, the channel bandwidth B is equal to 32 GHz. To calculate the SNR of each lightpath, first the launch power of the channels was optimised to maximise the average SNR, under the assumption that all channels are active, following the method described in [29]. Next, SNR for each channel— assuming full channel occupation — was calculated for a single span using a closed-form Gaussian noise model [30]. The SNR_z for each demand was then computed using the cumulative sum of the noise-to-signal ratio (NSR) across all spans s traversed by lightpath l in the i^{th} channel:

$$\text{NSR}_{i,l} = \sum_{s \in l} \text{NSR}_{i,s} \quad \textbf{(3)}$$

For the calculations above, a span length of $L_s = 80$ km and EDFA with a NF of 4.5 dB was assumed.

Previous work has shown an inverse correlation between throughput and path lengths [21]. Hence, the average length of established lightpaths is also included as a performance metric. Although additional metrics may be included. Two scenarios were evaluate in this work. In ***Scenario A***, network throughput and average path length were evaluated considering the same traffic demand used as input to the network expansion method. That is, the expanded network is not required to accommodate additional traffic but was tested only with all-to-all traffic used to determine the k edges. In ***Scenario B***, the network is stressed by increasing the number of connection demands. To do so, the Integer Linear Programming (ILP) proposed in [31] is used, where the objective function maximises the number of connection demands the network can accommodate subject to the standard constraints of optical networks. Scenario B allows us to evaluate the capability of the expanded network to adapt to future traffic growth.

A. Scenario A Results

We applied the proposed network expansion algorithms to 2 cases. The first considers 100 synthetic topologies [17] and the second includes 44 real-world topologies [32].

A.1. Case of Study 1: Synthetic topologies

For this case, the proposed network expansion algorithms received as input:

- 100 synthetic topologies generated by the SNR-BA method [17]. The SNR-BA method kept the number and location of the nodes of the NFSNet network (14 nodes and 21 edges), but varied the location of links from topology to topology.
- A traffic matrix where each node pair requires 1 connection, leading to a total of 182 demands ($|V| * (|V| - 1)$).
- The number of new edges, k: varied from 1 to 10 for each topology

For the expanded networks in this scenario, RWA was performed for all-to-all demands to calculate the delivered throughput. As mentioned earlier in this section, the Shannon capacity formula was used to determine the capacity of each demand based on the SNR of the occupied channel. Fig. 2(a) shows the average throughput (in Tbps) of the 100 expanded networks achieved by the proposed and baseline methods for different values of k, ($k = 0$ represents the original graphs). The exact throughput values are listed in Table 1, with the highest value highlighted in bold for each k. All proposed methods outperformed the baseline algorithms, with the hybrid algorithms achieving a slightly higher throughput than their CS counterparts. For example, for $k = 10$, MP3 + CS-G and MP3 + CS-SNR yielded 61.28 and 61.32 Tbps, respectively, as opposed to 60.93

and 61.08 Tbps for CS-G and CS-SNR, respectively. For the same type of method (hybrid or based on cut sets), SNR-aware strategies achieve better performance, highlighting the importance of incorporating aspects affecting throughput in the decision making. Notice how throughput increases due to the decreased path length and reduced SNR degradation, despite the traffic demands remaining unchanged. This highlights the significant impact of effective network expansion methods in efficiently accommodating demands.

For the given all-to-all demands, the average lightpath length was calculated for both the initial networks and the 100 expanded networks. Fig. 2(b) shows the average lightpath length of the same 100 networks normalised to the length of the longest lightpath in the original networks, for different values of k. The absolute values for the lightpath length for all-to-all demands (in number of spans traversed) are listed in Table 2, with the shortest length highlighted in bold for each k. The baseline algorithms show a path-length behaviour inversely correlated to throughput: they achieve the lowest throughput and also use the longest paths. For example, for $k = 10$, MP1 and DWC-based reduces path lengths by just 22% and 17% compared to reductions of 28% and 29% achieved by CS and hybrid methods, respectively. For values of $k \geq 5$, the expansion method MP3+CS-SNR shows the inverse correlation between path length and throughput: it achieves the highest throughput and, at the same time, the shortest path lengths. For $k \leq 4$ the method exhibiting the shortest paths is no longer the same achieving the highest throughput. However, the difference in path lengths is extremely small (in the first decimal position).

These results reveal two key findings. For $k \geq 5$ hybrid algorithms achieve best results, with MP3+CS-SNR achieving simultaneously highest average throughput and the shortest paths for the studied topologies. For lower values of k, the inverse correlation between throughput and path length is lost, with either MP3 + CS-SNR or CS-SNR achieving highest throughput but MP3 + CS-G or CS-G exhibiting shortest paths. However, the differences among the different methods are not significant in this case. The performance improvement when using a probabilistic method such as MP3+CS-SNR as k grows is not coincidental: the new edges to be added at low k values can be decided on using greedy approaches. As k grows, the number of edge-removal combinations grows exponentially. This combinatorial optimisation is difficult for greedy algorithms, however lends itself to a probabilistic-based optimisation method, such as the hybrid MP-methods.

A.2. Case of Study 2: Real-world topologies

For this case, the proposed network expansion algorithms received as input:

- 44 real-world topologies, extracted from [32] after discarding topologies including nodes with a nodal degree of 1. As shown in Table 3, each topology belongs to one of 3 clusters identified in [32].
- A traffic matrix where each node pair requires 1 connection, leading to a total of $|V| * (|V| - 1)$ demands.
- The number of new edges, k: varied from 1 to 5 for each topology

By analysing topologies belonging to different clusters,the relative performance of the explored network expansion methods can be evaluated in topologies with different structural, spatial, and spectral features. The goal of this analysis is to explore whether some types of networks benefit more - in terms of throughput - from edge additions and identify path-length and throughput correlations. For networks exceeding 20 nodes, the computationally simpler *Simple Path Search* method described in Section 2A was applied to find the cut sets. Among the 44 topologies analysed, the smallest topology contained 6 nodes, which led to the selection of $E_a = 7$ edges to ensure consistency across all networks. Additionally, the performance of the MP hybrid methods did not show significant differences when considering a smaller or larger number of E_a edges. Given the weaker performance observed for the baseline methods in the previous case study, this study focuses exclusively on the proposed methods. Unlike synthetic networks, real-world networks have different number of nodes and links, which complicates the comparison of throughput and path length problematic in terms of absolute values. Hence, for each network we calculated the ratio $\Delta T / T_{k=0}$, where $\Delta T = T_{k=i} - T_{k=0}$ is the difference between the throughput in the network extended with k new edges ($T_{k=i}$) and the throughput in the original network ($T_{k=0}$). Denoted as the *throughput increase ratio* it was used to calculate the average for all networks belonging to the same cluster. Figure 3(a) shows the average throughput increase ratio for the different network clusters as the number of new edges increases from 1 to 5. The impact of the network topology properties is clearly observed, with topologies in cluster 0 (solid lines) achieving a throughput increase ratio between 3 and 4 times higher than those in Cluster 1 (dashed lines) and 2 (dashed dot lines). Inside each cluster, CS-SNR achieves the best performance followed by MP3 + CS-SNR, CS-G and MP3 + CS-G, although the difference in performance among the different methods is negligible in Clusters 1 and 2.

Table 3. Real-world topologies. |T|: Number of topologies. |V|: Number of nodes. |E|: Number of edges. |δ|: Average node degree.

Cluster	|T|	|V|	|E|	|δ|
0	10	[19–75]	[23–99]	2.61
1	10	[6–13]	[6–14]	2.30
2	24	[12–50]	[16–88]	3.05

Similarly to the *throughput increase ratio*, we define the *lightpath length decrease ratio* as $\Delta L / L_{k=0}$, where $\Delta L = L_{k=0} - L_{k=i}$ is the difference between the lightpath length in the original network ($L_{k=0}$) and the lightpath length in the extended network ($L_{k=i}$). To explore the correlation between throughput and path length in real-world networks, we plotted the average lightpath length decrease ratio over all networks in the same cluster as a function of the number of new edges added in Figure 3(b). Apart from the impact of the topology on the lightpath length ratio, it is evident that the inverse correlation between throughput and lightpath length observed for the baseline methods in the synthetic topologies is no longer valid for topologies in clusters 0 (solid lines) and 1 (dashed lines). Whilst topologies in cluster 0 achieve the highest gain in throughput, they do not exhibit the highest decrease in lightpath lengths because of their network structural and physical properties. Similarly, whereas topologies in cluster 1 exhibited the highest decrease in lightpath length, they did not achieve the highest throughput gains. This behaviour has implications for the selection of metrics used as proxies of throughput (as done by the baseline algorithms), as they may not be adequate for certain types of topologies. Thus, the telecom operators needs to modify their network topology

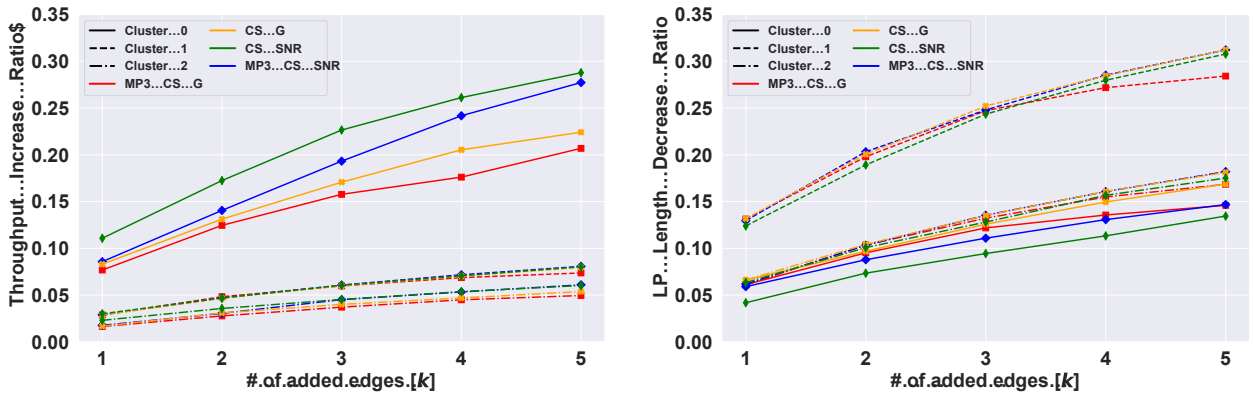

(a) (b)

Fig. 3. (a) Average throughput increase ratio and **(b)** average lightpath length decrease ratio for different clusters of real-world topologies.

gradually to fit in the clusters that achieve higher throughput.

These results lead to two key insights. Firstly, the relative performance of the methods in real-world topologies is similar to that observed in synthetic topologies: for low values of k CS-SNR achieves the highest throughput, with MP3 + CS-SNR closely following it or surpassing it as k increases. Secondly, the performance of optical network expansion methods is highly dependent on the network structural and physical properties. For example, the throughput performance of the different methods is difficult to differentiate in the synthetic topologies and clusters 1 and 2 of real-world topologies whilst CS-SNR has a clear advantage in topologies belonging to cluster 0 which have a lower average edge length. Additionally, topology has a strong impact on the design of network expansion methods. For example, methods using short path length as an indicator of high throughput will not deliver good results in cluster 1 and 2 topologies.

B. Scenario B Results:

In the previous section, we evaluated the throughput of synthetic and real-world extended networks assuming that the same set of traffic demands used to select the new edges will be in place after the network is extended. However, this is unrealistic. If a network is extended it will be expected to serve more traffic. Therefore, in this subsection we assess the performance of the extended synthetic networks when we maximise the number of connections they can accommodate by applying the ILP model presented in [31]. To do so, we first input each extended network to the ILP model in [31]. The ILP model outputs the maximum set of connections that can be accommodated in the extended network, for a given blocking probability (BP), with each connection associated with a route and a wavelength. This information is then used to evaluate the maximum achieved throughput using Eq. 2. Notice that due to the long runtimes of the ILP model, we only present results for the smaller 100 synthetic topologies with the number of nodes equal to 14 ($|V| = 14$) studied in subsection 3A.1 (Case of Study 1 in Scenario A). All results were obtained for BP=0%.

Fig. 4(a) and 4(b) show the maximum achievable throughput and the average lightpath length (measured in the number of spans) for the proposed network expansion methods as a function of k (number of edges added to the network). Compared to the results in Scenario A, the performance exhibited by the networks in Scenario B is significantly better: between $\times 4$ and $\times 9$ times higher throughput, with each new edge allowing - approximately - additional throughout of 50 Tbps for $k \leq 5$. Results also show that MP3 + CS-G achieved the worst throughput performance for all values of k. MP3 + CS-SNR achieved the highest throughput at $k \leq 4$, but loses this advantage to CS-G and CS-SNR at larger k values, although the difference in performance is small. For example, for $k = 10$ CS-G, CS-SNR and MP3 + CS-SNR achieved roughly $\times 2.6$, $\times 2.5$, and $\times 2.5$ higher throughput, respectively, than the original network ($k = 0$). In contrast, MP3 + CS-G achieved a throughput increase of approximately just $\times 2$ compared to the original network ($k = 0$). In terms of lightpath length, the cut set methods show a clear inverse correlation with throughput in this type of network, with CS-G and CS-SNR exhibiting the shortest average lengths when also achieving the highest values of throughput. This correlation is lost for the hybrid methods, as the selected edges, while reducing lightpath length, may not support bottleneck edges, potentially resulting in higher path lengths between demands in the network.

These results show that the consistently good performance of MP3 + CS-SNR for high values of k ($k \geq 4$) in cases where traffic demands are known (Scenario A) is lost in Scenario B, where the traffic pattern offered to the extended networks is unknown a priori. In this case, the cut set methods prove to be more effective in allowing more connection requests to be accommodated in the network. This advantage - although small - stems from the selection of edges that alleviate structural bottlenecks in the network, as opposed to a selection based on the input traffic. However, MP3 + CS-SNR remains competitive as it effectively decreases the impact of fibre nonlinearities on the demands by taking the SNR into account when selecting new edges. This directly contributes to achieving high throughput. In contrast, MP3 + CS-G consistently delivered low throughput. This difference arises because, although CS-G is used to identify a set E_a of edges to add, MP3 does not necessarily select the edge that alleviates the bottleneck (i.e. connects the subnetworks separated by the cut set) created for the different values of k. This is because the objective of MP3 inherently is to reduce the total

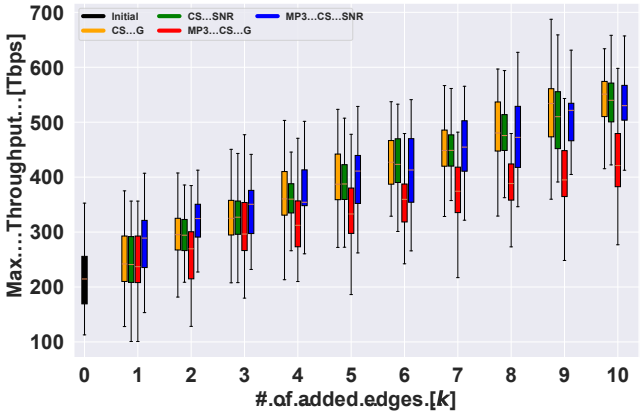

(a)

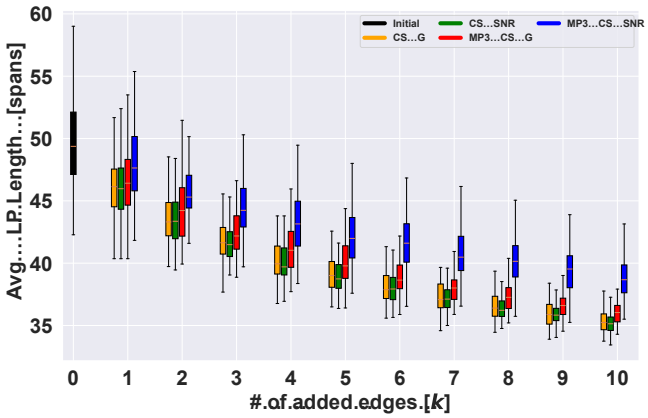

(b)

Fig. 4. (a) Delivered throughput and (b) Average lightpath length (measured in the number of spans) for the expanded networks at the $BP = 0\%$.

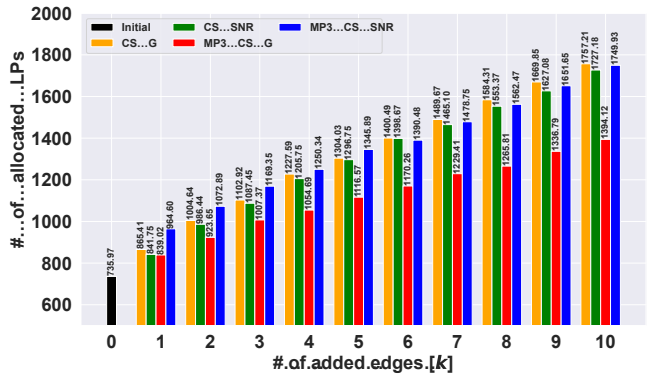

(a)

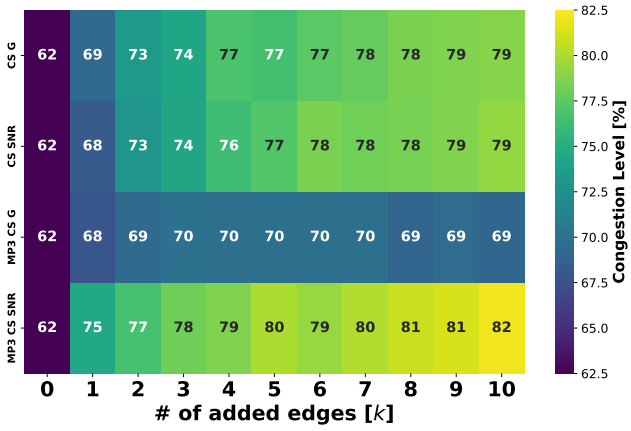

(b)

Fig. 5. (a) Average number of allocated lightpaths and (b) congestion level heatmap as a function of k for Scenario B.

path length within the network.

Given the similar performance of the methods, we investigated whether significant differences could be observed in terms of resource utilisation, specifically focusing on link congestion. Fig. 5(a) shows the average number of allocated lightpaths for all the proposed network expansion methods as a function of k (number of new edges). Aligned with the throughput results, across all k values, CS-G, CS-SNR and MP3 + CS-SNR allocate more lightpaths than MP3 + CS-G, with MP3 + CS-SNR accommodating slightly more lightpaths than the cut set methods for $k \leq 5$. After that threshold, CS-G achieved the highest number of allocated lightpaths. Furthermore, the selection of cut set edges plays a crucial role in traffic allocation, particularly as the network size grows, significantly influencing overall network capacity and efficiency. For instance, at $k = 1$, MP3 + CS-SNR allocated 15% more lightpaths than MP3 + CS-G (964 vs. 839) whilst at $k = 10$ CS-G allocated 26% more lightpaths than MP3 + CS-G (1757 vs. 1394).

Fig. 5(b) shows the heatmap of the average congestion level (percentage of wavelengths used per link) for varying values of k. The results are obtained by calculating the percentage of utilised wavelengths for each graph on the basis of the ILP results. Specifically, for each graph with $E = 21$ edges and $W = 156$ wavelengths per edge (resulting in a total of 21×156 wavelengths), the number of wavelengths assigned is divided by the total wavelength to determine the percentage of utilization. This process is repeated across 100 graphs for each value of k, and the average percentage is then computed. The figure highlights the improved link utilisation achieved by MP3 + CS-SNR, which increases by 20% at $k = 10$ compared to the initial networks with $k = 0$. CS-G and CS-SNR methods perform almost identically, increase wavelength occupancy by more than 16% at $k = 10$ with respect to the original network. In contrast, MP3 + CS-G shows a marginal improvement at an increase of more than 7% after adding 10 edges ($k = 10$) compared to the initial network.

We further investigated the length of the new edges added by the different proposed methods by quantifying the average number of amplifiers required after expansion. The average number of required amplifiers was calculated across the 100 graphs by summing the total edge lengths of each network and dividing by the span length, set to $L_s = 80km$. Fig. 6 shows these results. It can be seen that CS-G leads to longer edges than CS-SNR and MP3 + CS-SNR, resulting in a larger number of amplifiers. Thus, while these 3 methods (CS-G, CS-SNR, and MP3 + CS-SNR) demonstrate similar performance in terms of delivered throughput and the number of allocated lightpaths (and hence, number of transceivers required), CS-G does this at the expenses of a

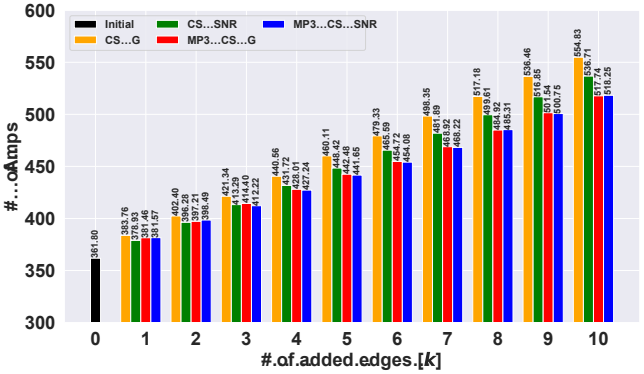

Fig. 6. Average number of optical amplifiers as a function of k

higher number of amplifiers. Based on this cost analysis, telecom operators can determine which method allows for cost-effective network growth while achieving higher capacity, helping them balance infrastructure investment with performance efficiency.

C. Computational Efficiency Analysis

Finally, we evaluated the execution time of the proposed methods for $k \in [1,5]$ in Scenario A. This was quantified using synthetically generated 6 random regular graphs with a degree of 3, ranging from 10 nodes with 15 edges to 100 nodes with 150 edges. Since these synthetic graphs require latitude and longitude data to calculate the edge lengths, the node locations were randomly selected within the European continent, within the latitude and longitude ranges of [35.0, 72.0] and [-25.0, 65.0], respectively.

In the case of the hybrid methods, the time required to obtain the set E_a was not included, as this set is part of the input data. Hence, we only use the name MP3 for the hybrid methods (as the difference between MP3 + CS-G and MP3 + CS-SNR lies in how the set E_a is built). If the time required to prepare the input data is considered, then the execution time of MP3 + CS-G and MP3 + CS-SNR is obtained by summing up the times of MP3 and the corresponding cut set method.

For the MP3 methods, the number of E_a edges was set equal to the number of nodes in the corresponding graph. For the cut set methods, the Simple Path Search was used to find the cut sets.

Table 4 shows the execution time of the methods for different graphs and values of k. The execution times were measured as wall-clock time using Python's `time.time()` function. As expected, the execution time grows with network size and the number of new edges for all methods, with CS-SNR exhibiting a significantly longer execution time compared to the CS-G and MP3, respectively. This is due to the need to solve the RWA problem for demands that grow quadratically with the number of nodes. This quadratic growth amplifies the number of calculations required, especially as the network size increases, making the execution time of CS-SNR much longer. The MP3 procedure is the fastest for the 4 smallest networks, quickly surpassing the time of CS-G for larger networks. However, MP3 needs a set of E_a edges as input data. Thus, depending on whether CS-G or CS-SNR is used for this task, MP3 + CS-G and MP3 + CS-SNR are likely to exhibit the second shortest execution time (after CS-G) or the longest execution time, respectively.

Table 4. Computation times (in seconds) for CS G, MP3, and CS SNR network expansion methods across different graph sizes.

$(\|V\|,\|E\|)$	k	CS G	MP3	CS SNR
(10,15)	1	55.58	**1.96**	285.34
	2	111.72	**2.11**	553.12
	3	168.41	**3.70**	825.62
	4	226.05	**5.38**	1088.83
	5	284.26	**6.98**	1360.53
(28,42)	1	468.21	**45.17**	2561.01
	2	938.28	**51.95**	5251.73
	3	1420.59	**91.32**	7716.41
	4	1906.25	**137.36**	10117.10
	5	2394.17	**181.48**	12664.40
(46,69)	1	1300.41	**506.00**	9599.22
	2	2584.72	**710.70**	18767.75
	3	3875.19	**1010.63**	28226.46
	4	5175.39	**1531.50**	37227.96
	5	6488.66	**2038.00**	45939.18
(64,96)	1	2534.25	**2642.00**	26434.09
	2	5090.99	**3261.42**	50681.26
	3	7638.77	**5489.00**	77052.33
	4	10224.08	**8509.00**	102182.25
	5	12826.02	**11743.00**	129906.54
(82,123)	1	**4310.73**	8447.00	57813.85
	2	**8651.02**	10837.00	115652.54
	3	**12956.45**	16650.00	173491.23
	4	**17273.50**	24532.00	231329.93
	5	**21680.55**	32756.00	289168.62
(100,150)	1	**6760.98**	28861.00	118505.85
	2	**13433.56**	38015.92	243693.33
	3	**20242.43**	59408.00	369389.73
	4	**27354.10**	91023.00	492724.74
	5	**34152.21**	120494.00	583467.79

4. CONCLUSION

In this paper, we proposed 4 novel optical network growth methods for maximum throughput and applied them to 100 NSFNET-based synthetic networks and 44 real-world network topologies clustered in 3 categories. The results show three main trends. First, expansion methods considering the SNR (CS-SNR and MP3 + CS-SNR) achieved the best performance in all scenar-

ios and types of topologies and decreased the average lightpath length by 29% for the all-to-all demands and increased the maximum achievable throughput by more than $\times 2.5$ times for the 100 synthetic optical networks by adding $k = 10$ edges. The algorithm MP3 + CS-SNR selects shorter links which makes it more efficient and cost-effective in terms of amplifier requirements. This results in approximately 36 fewer amplifiers compared to other greedy CS-SNR methods for $k = 10$. Second, although the SNR-based methods are the slowest, scaling poorly with network size, network expansion does not need to be solved in short timescales and thus, execution time may be a less important consideration. Finally, the inverse correlation between network throughput and lightpath length assumed by some methods, is not valid in all topologies. As a result, expansion methods relying on minimising lightptah lengths do not generalise well across topologies. Overall, this study has, for the first time, explored network growth in optical transmission networks, demonstrating that to evolve an existing network to increase its throughput with minimal cost, it is important to account for both the structural and physical properties of the network. The combination of CS-SNR and MP3 (MP3 + CS-SNR) achieved this by identifying the most effective set of edges to add to the network to have the greatest impact on network throughput.

ACKNOWLEDGEMENTS

Financial support from the EPSRC TRANSNET Programme Grant (EP/R035342/1) is gratefully acknowledged. Polina Bayvel is additionally supported by a Royal Society Research Professorship.

REFERENCES

1. "Cisco CAGR prediction 2018-2023," https://www.cisco.com/c/en/us/solutions/collateral/executive-perspectives/annual-internet-report/white-paper-c11-741490.html.
2. H. Buglia, R. I. Killey, and P. Bayvel, "Ultra-wideband modelling of optical fibre nonlinearity in hybrid-amplified links," J. Light. Technol. (2024).
3. T. Hoshida, V. Curri, L. Galdino, D. T. Neilson, W. Forysiak, J. K. Fischer, T. Kato, and P. Poggiolini, "Ultrawideband systems and networks: Beyond c+ l-band," Proc. IEEE **110**, 1725–1741 (2022).
4. E. Agrell, M. Karlsson, F. Poletti, S. Namiki, X. V. Chen, L. A. Rusch, B. Puttnam, P. Bayvel, L. Schmalen, Z. Tao, F. R. Kschischang, A. Alvarado, B. Mukherjee, R. Casellas, X. Zhou, D. van Veen, G. Mohs, E. Wong, A. Mecozzi, M.-S. Alouini, E. Diamanti, and M. Uysal, "Roadmap on optical communications," J. Opt. **26**, 093001 (2024).
5. R. Sadeghi, B. Correia, A. Souza, N. Costa, J. Pedro, A. Napoli, and V. Curri, "Transparent vs translucent multi-band optical networking: Capacity and energy analyses," J. Light. Technol. **40**, 3486–3498 (2022).
6. P. S. Khodashenas, J. M. Rivas-Moscoso, D. Siracusa, F. Pederzolli, B. Shariati, D. Klonidis, E. Salvadori, and I. Tomkos, "Comparison of spectral and spatial super-channel allocation schemes for sdm networks," J. Light. Technol. **34**, 2710–2716 (2016).
7. F. Pederzolli, D. Siracusa, B. Shariati, J. M. Rivas-Moscoso, E. Salvadori, and I. Tomkos, "Improving performance of spatially joint-switched space division multiplexing optical networks via spatial group sharing," J. Opt. Commun. Netw. **9**, B1–B11 (2017).
8. R. Matzner, H. Buglia, and P. Bayvel, "Evolving optical core networks: understanding the impact of topology redesign using space and wavelength domains on network throughput," in *49th European Conference on Optical Communications (ECOC 2023),* vol. 2023 (2023), pp. 1043–1046.
9. D. Saito, Y. Mori, K. Hosokawa, S. Yanagimachi, and H. Hasegawa, "Cost-effective capacity enhancement of survivable optical networks by supplemental band expansion and backup resource sharing," in *2024 Optical Fiber Communications Conference and Exhibition (OFC),* (2024), pp. 1–3.
10. B. Correia, R. Sadeghi, E. Virgillito, A. Napoli, N. Costa, J. Pedro, and V. Curri, "Power control strategies and network performance assessment for c+l+s multiband optical transport," J. Opt. Commun. Netw. **13**, 147–157 (2021).
11. M. Tornatore, G. Maier, and A. Pattavina, "WDM Network Design by ILP Models Based on Flow Aggregation," IEEE/ACM Transactions on Netw. **15**, 709–720 (2007).
12. R. Matzner, H. Buglia, and P. Bayvel, "Evolving optical core networks: understanding the impact of topology redesign using space and wavelength domains on network throughput," in *49th European Conference on Optical Communications (ECOC 2023),* vol. 2023 (2023), pp. 1043–1046.
13. R. Luo, R. Matzner, A. Ottino, G. Zervas, and P. Bayvel, "Exploring the relationship among traffic, topology, and throughput: towards a traffic-optimal optical network topology design," J. Opt. Commun. Netw. **15**, B1–B10 (2023).
14. A. Ahuja, S. N. Herzberg, A. Rafel, P. Wright, A. Lord, and S. J. Savory, "Topology-driven edge predictions with graph machine learning for optical network growth," in *Optical Fiber Communication Conference,* (Optica Publishing Group, 2024), pp. M1H–5.
15. V.-A. Darvariu, S. Hailes, and M. Musolesi, "Planning spatial networks with monte carlo tree search," Proc. Royal Soc. A **479**, 20220383 (2023).
16. M. Zhang, "Graph neural networks: link predictions," Graph Neural Networks: Foundations, Front. Appl. pp. 195–223 (2022).
17. R. Matzner, D. Semrau, R. Luo, G. Zervas, and P. Bayvel, "Making intelligent topology design choices: understanding structural and physical property performance implications in optical networks [invited]," J. Opt. Commun. Netw. **13**, D53–D67 (2021).
18. R. Luo, R. Matzner, G. Zervas, and P. Bayvel, "Towards a traffic-optimal large-scale optical network topology design," in *2022 International Conference on Optical Network Design and Modeling (ONDM),* (IEEE, 2022), pp. 1–3.
19. E. Virgillito, R. Sadeghi, A. Ferrari, A. Napoli, B. Correia, and V. Curri, "Network performance assessment with uniform and non-uniform nodes distribution in c+l upgrades vs. fiber doubling sdm solutions," in *2020 International Conference on Optical Network Design and Modeling (ONDM),* (2020), pp. 1–6.
20. Y.-Z. Xu and D. Saad, "Network pruning and growth: Probabilistic optimization," Phys. Rev. Res. **5**, 033087 (2023).
21. R. Sadeghi, R. Matzner, Y.-Z. Xu, A. Beghelli, D. Saad, and P. Bayvel, "Maximising throughput through demand-aware optical network growth," in *ECOC 2024; 50th European Conference on Optical Communication,* (2024), pp. 994–997.
22. K. Hayashi, Y. Mori, and H. Hasegawa, "Efficient network capacity expansion by differentiated wdm-density with bandwidth-variable virtual direct links," in *2022 IEEE Future Networks World Forum (FNWF),* (2022), pp. 310–313.
23. K. Hayashi, Y. Mori, and H. Hasegawa, "Cost-effective network capacity upgrade by heterogeneous wavelength division multiplexing density with bandwidth-variable virtual direct links," J. Opt. Commun. Netw. **15**, D23–D32 (2023).
24. M. Opper and D. Saad, *Advanced mean field methods : theory and practice*, Neural information processing series (MIT Press, Cambridge, Mass, 2001).
25. C. H. Yeung and D. Saad, "Competition for shortest paths on sparse graphs," Phys. Rev. Lett. **108**, 208701 (2012).
26. C. H. Yeung, D. Saad, and K. Y. M. Wong, "From the physics of interacting polymers to optimizing routes on the london underground," Proc. Natl. Acad. Sci. **110**, 13717–13722 (2013).
27. Y.-Z. Xu, H. F. Po, C. H. Yeung, and D. Saad, "Scalable node-disjoint and edge-disjoint multiwavelength routing," Phys. Rev. E **105**, 044316 (2022).
28. S. Baroni, P. Bayvel, and R. J. Gibbens, "On the number of wavelengths in arbitrarily-connected wavelength-routed optical networks," in *Optical Networks and Their Applications,* (Optica Publishing Group, 1998), p.

MN2.
29. M. Jarmolovičius, D. Semrau, H. Buglia, M. Shevchenko, F. M. Ferreira, E. Sillekens, P. Bayvel, and R. I. Killey, "Optimising o-to-u band transmission using fast isrs gaussian noise numerical integral model," J. Light. Technol. **42**, 7095–7103 (2024).
30. D. Semrau, R. I. Killey, and P. Bayvel, "A closed-form approximation of the gaussian noise model in the presence of inter-channel stimulated raman scattering," J. Light. Technol. **37**, 1924–1936 (2019).
31. R. Matzner, R. Luo, G. Zervas, and P. Bayvel, "Intelligent performance inference: A graph neural network approach to modeling maximum achievable throughput in optical networks," APL Mach. Learn. **1**, 026112 (2023).
32. R. Matzner, A. Ahuja, R. Sadeghi, M. Doherty, A. Beghelli, S. J. Savory, and P. Bayvel, "Topology bench: systematic graph-based benchmarking for core optical networks," J. Opt. Commun. Netw. **17**, 7–27 (2025).
33. R. Diestel, *Graph Theory: 6th edition* (Springer (print edition); Reinhard Diestel (eBooks), 2024).

A. APPENDIX: NETWORK EXPANSION METHODS

A. Algebraic Connectivity Based Method

In this method, we evaluated the potential impact of each candidate edge on the network overall connectivity by examining the algebraic connectivity, also known as the Fiedler value, of the graph [33]. The algebraic connectivity is the second smallest eigenvalue of the graph's Laplacian matrix L. For a given graph $G(V, E)$, the Laplacian matrix L is defined as:

$$L = \Delta - A \tag{4}$$

where Δ is the degree matrix (a diagonal matrix where each diagonal element represents the degree of a corresponding node) and A is the adjacency matrix of the graph. The eigenvalues of the Laplacian matrix, $\lambda_1 \leq \lambda_2 \leq \cdots \leq \lambda_n$, provide critical insights into the graph's connectivity. Specifically, λ_2, the second smallest eigenvalue, is known as the algebraic connectivity.

For each candidate edge, we compute the new algebraic connectivity after hypothetically adding the edge to the graph. The edge that results in the highest increase in λ_2 is selected, as this indicates a better-connected network. This process is repeated iteratively until k edges are identified.

B. Message Passing methodology

The MP approach can be cast as a minimisation of a cost function (e.g., latency, throughput) under some problem constraints, such as that routing assignments should be contiguous from source to destination. Two types of variables are introduced in this model, one for routing assignment optimisation ($\sigma^{\mu}_{i,j}$) and the other for edge addition ($c_{i,j}$), in which $\sigma^{\mu}_{i,j} = \pm 1$ if route assignment μ passes through edge (i, j), from node i to node j ($\sigma^{\mu}_{i,j} = 1$) or the other way around ($\sigma^{\mu}_{i,j} = -1$), and $\sigma^{\mu}_{i,j} = 0$ otherwise. Routing and edge addition are combined into one cost function (Hamiltonian in the statistical physics literature) given by

$$H(\{\vec{\sigma}^{\mu}\}, \vec{c}) = \sum_{\mu} \sum_{(i.j)} w_{i,j} |\sigma^{\mu}_{i,j}| + \lambda \sum_{(i,j)} c_{i,j}, \tag{5}$$

where λ is a Lagrange multiplier controlling the number of edges to be added, $w_{i,j}$ is the weight, length or delay of edge (i, j), $\vec{\sigma}^{\mu} \equiv (\ldots, \sigma^{\mu}_{i,j}, \ldots)$; $c_{i,j} = 1$ if edge (i, j) is added to the network and 0 otherwise. Additionally, the routing variables $\sigma^{\mu}_{i,j}$ are restricted by the path continuity of assignment μ. According to Boltzmann distribution in equilibrium statistical physics $p(\{\vec{\sigma}^{\mu}\}, \vec{c}) \propto \mathrm{e}^{-\frac{1}{T} H(\{\vec{\sigma}^{\mu}\}, \vec{c})}$, we can find the shortest path of each assignment when the temperature parameter (T) is low enough, and consequently the optimal k edges can be found by the MP algorithm, which has the computational complexity $O(|D|^2 |E|(|E_a| - k))$.

MP3 is an algorithm for network expansion under the simplest routing assignment scenario where no interaction between routing assignments exists and the Hamiltonian or cost function is given by Eq. (5). Following the derivation of [20], the marginal probability of the edges in E_a to be added can be calculated by:

$$r_{i,j} = \frac{\mathrm{e}^{-\beta\lambda}}{\mathrm{e}^{-\beta\lambda} + \prod_{\mu} \tilde{r}^{\mu}_{i,j}(0)}, \tag{6}$$

where $\beta (\equiv 1/T)$ is the inverse temperature which can be treated as a predetermined parameter, $\tilde{r}^{\mu}_{i,j}(0)$ is the probability that routing assignment μ does not pass through edge (i, j) irrespective of the influence of edge state $c_{i,j}$ ($c_{i,j} = 1$ if added, $c_{i,j} = 0$ otherwise); the product $\prod_{\mu} \tilde{r}^{\mu}_{i,j}(0)$ means that no routing assignment uses edge (i, j), so that the edge should not be added. $\mathrm{e}^{-\beta\lambda}$ is the probability that edge (i, j) should be added, where λ is the corresponding cost.

At the heart of message passing is the calculation of variable fields *in the absence of the one considered, termed the cavity field* in statistical physics. This eventually is being used to calculate the marginal posterior probability for the variable values. In the routing related cavity probability $\tilde{r}_{i,j}(\sigma^{\mu}_{i,j}) \propto \mathrm{e}^{-\beta w_{i,j} |\sigma^{\mu}_{i,j}|} p^{\mu}_{i\to j}(\sigma^{\mu}_{i,j}) p^{\mu}_{j\to i}(-\sigma^{\mu}_{i,j})$ for routing assignment μ using edge (i, j) without considering the influence of the edge state $c_{i,j}$; $p^{\mu}_{i\to j}(\sigma^{\mu}_{i,j})$ is the cavity probability of edge (i, j) being in state $\sigma^{\mu}_{i,j}$ with node i supporting routing assignment μ, and edge weight $w_{i,j}$ contributes to the total cost if edge (i, j) being part of the route for assignment μ, in other words $\sigma^{\mu}_{i,j} = \pm 1$. The message probability $p^{\mu}_{i\to j}(\sigma^{\mu}_{i,j})$ (for brevity we will use the dummy state variable σ) is obtained from the closed set of MP equations:

$$\begin{cases} p^{\mu}_{i\to j}(0) \propto \displaystyle\prod_{k\in\partial i\setminus j} q^{\mu}_{k\to j}(0) \\ \qquad\qquad + \displaystyle\sum_{m,n\in\partial i\setminus j} q^{\mu}_{m\to i}(1) q^{\mu}_{n\to i}(-1) \prod_{k\in\partial i\setminus m,n,j} q^{\mu}_{k\to i}(0), \\ p^{\mu}_{i\to j}(\pm 1) \propto \displaystyle\sum_{k\in\partial i\setminus j} q^{\mu}_{k\to i}(\pm 1) \prod_{l\in\partial i\setminus j,k} q^{\mu}_{l\to i}(0), \\ q^{\mu}_{i\to j}(\sigma) \propto \mathrm{e}^{-\beta w_{i,j}|\sigma|} r^{\mu}_{i,j}(\sigma) p^{\mu}_{i\to j}(\sigma), \\ r^{\mu}_{i,j}(0) \propto \displaystyle\prod_{\nu\neq\mu} \tilde{r}^{\nu}_{i,j}(0) + \mathrm{e}^{-\beta\lambda}, \quad r^{\mu}_{i,j}(\pm 1) \propto \mathrm{e}^{-\beta\lambda}, \end{cases} \tag{7}$$

where the proportionality symbol $\propto$ is used to avoid the normalisation terms for brevity; $\partial i \setminus j$ is the nearest neighbouring node set of i except j, $q^{\mu}_{i\to j}(\sigma)$ is the probability of edge (i, j) being in state σ without the influence of node j on routing assignment μ, and $r^{\mu}_{i,j}(\sigma)$ is the probability of $\sigma^{\mu}_{i,j} = \sigma$ given the state $c_{i,j}$. The first term in the first equation of Eq. (7) represents the case where routing assignment μ does not go through node i, and the second term where it does, through $m \to i \to n$; in the second equation, routing assignment μ passes through edge (i, j) through $i \to j$ (or $j \to i$) and another edge (k, i) through $k \to i$ (or $i \to k$). To close the equations, there is another equation for λ, representing the total added edges constraint, which is determined by:

$$\sum_{(i,j)\in E_a} r_{i,j} = k. \tag{8}$$

One can obtain the value of λ by solving this equation.

B.1. MP3 algorithm

The steps of the message passing algorithm for edge addition are as follows:

0. read the network with weights $G(V, E, W)$ combined with the candidate edge set E_a and the demand list D; set β to a large positive value, set the number of edges to be added k; and randomly initialise the messages/probabilities $\{p^{\mu}_{\to}, q^{\mu}_{\to}\}$ and λ;

1. update the messages by the MP equations Eq. (7) and the value of λ a predefined number of times, then calculate the marginal probability $r_{i,j}$ by Eq. (6);

Table 5. Average lightpath length, measured in the number of spans, for methods in the appendix across 100 initial graphs, with k edges added (ranging from 1 to 10) for the all to all traffic pattern. The average lightpath length for the initial networks is equal to 41 spans.

k=	1	2	3	4	5	6	7	8	9	10
MP2_SNR_max	38.34	36.47	35.55	34.59	33.83	33.18	32.83	32.40	32.04	31.85
Algebraic Connectivity	39.19	38.05	36.95	36.19	35.31	34.70	34.15	33.55	33.10	32.67
MP2_SNR_max CS G	39.38	36.74	35.54	34.42	33.55	32.72	31.95	31.32	30.76	30.21
MP2_SNR_max CS SNR	39.59	36.80	35.57	34.57	33.43	32.72	32.02	31.28	30.67	30.10

Table 6. Average network capacity (Tbps) for methods in the appendix across 100 initial graphs, with k edges added (ranging from 1 to 10) for the all to all traffic pattern. The initial 100 networks delivered capacity for all to all demands is equal to 56.01 Tbps.

k=	1	2	3	4	5	6	7	8	9	10
MP2_SNR_max	56.87	57.54	57.92	58.33	58.72	59.04	59.21	59.46	59.65	59.77
Algebraic Connectivity	56.58	57.01	57.43	57.75	58.13	58.43	58.71	59.02	59.26	59.49
MP2_SNR_max CS G	56.58	57.46	57.97	58.47	58.88	59.30	59.67	60.01	60.33	60.65
MP2_SNR_max CS SNR	56.53	57.47	57.97	58.44	58.95	59.30	59.71	60.06	60.40	60.73

2. fix the state $c_{i,j} = 0$ for the edge with the smallest probability $r_{i,j}$ in E_a and remove it to simplify the network;

3. do step 1 and step 2 $(|E_a| - k)$ times, and output the E_a edges in the residual network.

B.2. MP1 and MP2

MP1 and MP2 are variants of MP3 with more realistic details, where edge-disjoint (each edge on each wavelength can be occupied by at most one routing assignment) on multi-wavelength network is considered. The equations have to be modified, e.g. Eq. (6) should be adjusted to:

$$r_{i,j} = \frac{\mathrm{e}^{-\beta\lambda}}{\mathrm{e}^{-\beta\lambda} + \prod_{a,\mu} \tilde{r}_{i,j}^{a,\mu}(0)}, \tag{9}$$

where a is the wavelength label and $\tilde{r}_{i,j}^{a,\mu}(0)$ represents the probability that routing assignment) μ does not use edge (i,j) on wavelength a without the influence of the state $c_{i,j}$. Multi-wavelength routing is resolved by generalising the routing variable $\sigma_{i,j}^{\mu}$ to $\{\sigma_{i,j}^{a,\mu}\}_a$; edge-disjoint is settled through introducing additional interactions (factor nodes in the MP terminology) that capture the probability of using wavelength a on edge (i,j) for routing assignment μ in the form

$$\begin{cases} t_{i,j}^{a,\mu}(0) \propto \prod\limits_{\nu\neq\mu} \tilde{t}_{i,j}^{a,\mu}(0) + \mathrm{e}^{-\beta w_{i,j}^{a}} \sum\limits_{\nu\neq\mu} \tilde{t}_{i,j}^{a,\nu}(1) \prod\limits_{\omega\neq\mu,\nu} \tilde{t}_{i,j}^{a,\omega}(0), \\ t_{i,j}^{a,\mu}(1) \propto \mathrm{e}^{-\beta w_{i,j}^{a}} \prod\limits_{\nu\neq\mu} \tilde{t}_{i,j}^{a,\nu}(0), \end{cases} \tag{10}$$

where $\tilde{t}_{i,j}^{a,\mu}(c)$ is the probability that wavelength a on edge (i,j) being used by routing assignment μ $(c = 1)$ or not if $(c = 0)$, and edge weights $w_{i,j}^{a} = w_{i,j}$ in MP1. The first equation in Eq. (10) is that wavelength a on edge (i,j) is not used by any routing assignment, or used by one routing assignment ν and have the cost contribution $w_{i,j}^{a}$, whereas the second equation shows the case where routing assignment μ takes wavelength a on edge (i,j) only. The other equations and algorithm framework are similar to those of MP3; additional details can be found in Ref. [20].

In the second variant of the message-passing method, referred to as MP2, we extended the approach used in MP1 by considering SNR values as edge weights instead of distances. This modification was introduced to account for nonlinearities in the network topology expansion process. By using SNR, MP2 prioritised the selection of edges that maximised throughput in the resulting network topology compared to the MP1 method. for example, delivered throughput for all to all demands at $k = 10$ based on this method is 59.77 Tbps which is slightly higher than MP1 method for the same k value. In this scenario, we have considered the simple greedy method to select the E_a edges. Then, to improve the performance of the second variant of this method, the CS G and CS SNR greedy methods have been utilized in the selection of E_a edges process (namely MP2_SNR_max_CS G and MP2_SNR_max_CS SNR). According to this table, the achieved throughput for all to all demands increased from 59.77 Tbps (MP2_SNR_max) to 60.65 Tbps (MP2_SNR_max CS G) and 60.73 Tbps (MP2_SNR_max CS SNR) at $k = 10$. In tables 5 and 6 the average lightpath length and delivered throughput for all to all demands have been summarised for all proposed methods in this appendix.